

Constraining ALP-Top Interaction from the Chromoelectric Dipole Moment of the Top Quark

Subhadip Bisal^{a,b}

^a *School of Physical Sciences, Indian Association for the Cultivation of Science, 2A & 2B, Raja S.C. Mullick Road, Jadavpur, Kolkata 700032, India*

^b *School of Physics, Zhengzhou University, Zhengzhou 450000, China*

E-mail: subhadipbisal6@gmail.com

ABSTRACT: The couplings of axion-like particles (ALPs) to fermions are proportional to the fermion masses, making the interaction with the top quark particularly significant. In this study, we consider an ALP that is a mixture of CP-even and CP-odd components, thereby introducing CP violation. This CP violation, in turn, gives rise to electric dipole moments (EDMs) of quarks and leptons, as well as chromoelectric dipole moments (CEDMs) of quarks. We compute the one-loop and two-loop contributions to the top quark CEDM induced by the ALP. In our calculation, we treat the external gluon as off-shell with momentum $q^2 \neq 0$, derive the analytical results, and finally evaluate the top quark CEDM at $q^2 = m_t^2$, corresponding to the top quark pole mass. This value is relevant for subsequent calculations of the EDMs of the neutron and mercury. By applying current experimental bounds on EDMs and CEDMs, we derive constraints on the ALP-top quark coupling, with the strongest limit coming from the neutron EDM.

Contents

1	Introduction	1
2	The CP-Violating ALPs	3
3	The Chromoelectromagnetic Dipole Moment	4
4	Calculation of the Top Quark CEDM	5
4.1	One-loop contribution	5
4.2	Two-loop contribution	6
5	Contribution to the Weinberg Operator, Neutron EDM, and Mercury EDM	8
6	Constraints on ALP-Top Quark Coupling from Other Searches	10
7	Constraints on ALP-Top Coupling from Top Quark CEDM, Neutron EDM, and Mercury EDM	11
8	Summary and Conclusions	14
9	Acknowledgements	14
A	Two-Loop Form Factors	14

1 Introduction

The lack of discoveries related to heavy new physics at the Large Hadron Collider (LHC), which was largely anticipated due to the weak-scale hierarchy problem, has encouraged a change in direction. As a result, scenarios featuring light mediators are gaining growing attention in both theoretical studies and experimental searches. Light spin-0 particles, whether scalar, pseudoscalar or a combination of both, are often collectively known as axion-like particles (ALPs). These types of particles frequently arise in theories beyond the Standard Model (SM). Their small mass, when compared to the typical scale of new physics, can often be attributed to their nature as pseudo-Nambu-Goldstone bosons, meaning they are associated with an underlying broken symmetry. ALPs represent a broader class of particles that includes the well-known QCD axion, but differ in that their mass and couplings are free parameters, subject to experimental constraints. Interestingly, ALPs offer possible solutions to several fundamental questions in particle physics. These include the strong CP problem [1–4], the nature and origin of dark matter [5–8], and the unresolved issues related to flavor [9–12] and mass hierarchies [13].

The search for ALPs with masses below the MeV scale has spurred a wide array of experimental efforts, many of which intersect with astrophysical and cosmological studies [14–17]. In the sub-eV range, experiments employ *wave-based* detection techniques such as haloscopes, helioscopes, and optical setups, while beam-dump experiments extend sensitivity up to the GeV scale [18]. At higher energies, collider experiments have probed ALP masses from the GeV level to the electroweak (EW) scale by analyzing their associated production with photons, jets, and EW bosons [19–25]. Furthermore, searches for exotic on-shell Z boson and Higgs decays into ALPs have revealed previously unexplored regions of the parameter space [26, 27].

Interestingly, CP-violating signatures of ALPs have received relatively little attention so far [28–35]. The CP symmetry is violated when the ALP (a) couples to fermions (ψ_f) via a combination of scalar or CP-even ($a\bar{\psi}_f\psi_f$) and pseudoscalar or CP-odd ($a\bar{\psi}_f\gamma_5\psi_f$) operators.¹ If ALPs exhibit CP-violating interactions, they could induce fermion electric dipole moments (EDMs) [28, 36]. Similar to leptons and quarks possessing an EDM, quarks can also acquire chromoelectric dipole moments (CEDMs) through their interactions with external gluon fields.

The top quark holds a unique position in the study of the SM phenomenology. This is because its mass is approximately the same as the EW symmetry breaking (EWSB) scale. Unlike other quarks, the top quark is unique because its very short lifetime (5×10^{-25} sec) prevents it from hadronizing. Instead, it decays semi-weakly and has a Yukawa coupling of $\mathcal{O}(1)$. At a center-of-mass (c.o.m) energy of $\sqrt{s} = 14$ TeV, approximately 90% of top quark production results from gluon fusion ($gg \rightarrow t\bar{t}$), with the remaining fraction comes from $q\bar{q}$ annihilation [37]. Therefore, unlike the lepton EDM, which is measured in low-energy experiments (e.g., atomic/molecular spectroscopy), the top quark CEDM, however, can only be measured dynamically in high-energy collisions. In many beyond the SM (BSM) scenarios, the CEDM has been studied at the one-loop level in the presence of CP-violating interactions (see, e.g., Refs. [36, 38–45]). Similarly, two-loop contributions to the CEDM have also been studied in various BSM contexts (see, e.g., Refs. [36, 44–48]).

The current experimental upper limit on the CEDM of top quark is [49]

$$\left| \tilde{d}_t^C \right|_{\text{Exp.}} < 0.03 \text{ at 95\% confidence level (C.L.).} \quad (1.1)$$

This constraint is derived from measurements of the chromomagnetic dipole moment (CMDM) of top quark by the CMS collaboration at the LHC, using pp collisions with a c.o.m energy of 13 TeV and an integrated luminosity of 35.9 fb^{-1} [49].

In this study, we calculate the CEDM of the top quark mediated by an ALP. Focusing on CP-violating ALP-top quark interactions, we demonstrate how these induce a CEDM. We perform computations at both one-loop and two-loop levels, with the two-loop contribution originating from a Barr-Zee-type diagram. As has already been stated, the CEDM of the top quark can only be measured at high energies, we account for this by considering the external gluon to be off-shell, i.e., carrying a nonzero momentum transfer ($q^2 \neq 0$). We

¹The CP symmetry is also broken when the ALP-photon coupling includes both $aF_{\mu\nu}\tilde{F}^{\mu\nu}$ and $aF_{\mu\nu}F^{\mu\nu}$ interactions, where $F^{\mu\nu}$ is the electromagnetic field strength tensor and $\tilde{F}^{\mu\nu}$ denotes its dual.

perform a complete two-loop computation and present the analytical formulae for the form factors contributing to the top quark CEDM for $q^2 \neq 0$. We then evaluate the numerical values at the top quark pole mass, i.e., at $q^2 = m_t^2$. To the best of my knowledge, this result is not available in the existing literature. We further extend our analysis to determine the contribution of the top quark CEDM to the Weinberg operator, as well as to the EDMs and CEDMs of light quarks, which are induced via the top CEDM. Using these results, we then compute the EDMs of the neutron and mercury, both of which crucially depend on the top quark CEDM evaluated at its pole mass. Finally, employing the current experimental bounds on the top quark CEDM (see Eq. (1.1)) and the limits on the neutron and mercury EDMs, we derive constraints on the ALP-top coupling.

The paper is structured as follows. In Sec. 2, we provide a brief introduction to the CP-violating ALPs and their couplings to fermions. Sec. 3 discusses the CEDM, EDM, and the Weinberg operator within the effective Lagrangian framework. We then present the one-loop calculation and a detailed two-loop calculation of the top quark CEDM mediated by the ALP in Sec. 4, maintaining full generality. In Sec. 5, we analyze the impact of the top quark CEDM on the Weinberg operator, as well as on the neutron and mercury EDMs. Sec. 6 summarizes existing constraints on the ALP-top coupling from collider searches (CMS, ATLAS) and low-energy precision experiments (NA62, BABAR). Our main results, including limits on the ALP-top coupling derived from top quark CEDM, neutron EDM, and mercury EDM, are presented in Sec. 7. Finally, we conclude with a summary of our findings in Sec. 8.

2 The CP-Violating ALPs

The ALP exhibits a broad spectrum of possible couplings. In this work, we focus exclusively on the standard CP-even and CP-odd interactions between the ALP, denoted as a , and fermions ψ_f , which induce CP-violating effects. These interactions give rise to EDMs of leptons and quarks, as well as CEDMs of quarks. Additional couplings, such as those between the ALP and gauge bosons, can be generated at loop level. The effective Lagrangian describing the ALP-fermion interaction takes the following form [28, 33, 36, 50–53]:

$$\mathcal{L}^a = - \sum_{\psi_f} \frac{m_f}{f_a} c_f a \bar{\psi}_f \psi_f - \sum_{\psi_f} i \frac{m_f}{f_a} \tilde{c}_f a \bar{\psi}_f \gamma_5 \psi_f, \quad (2.1)$$

where m_f represents the mass of the fermion f , while c_f and \tilde{c}_f are the real parameters. The quantity f_a corresponds to a heavy new scale, with $f_a \gg v$, where $v = 246$ GeV denotes the EW scale. In Eq. (2.1), the first term is CP-even while the second term is CP-odd. Therefore, the combination of these terms violates CP. The pseudoscalar interactions (CP-odd) can be expressed in a shift-symmetric form using the dimension-five operator $\sim \frac{\partial_\mu a}{2f_a} (\bar{f} \gamma^\mu \gamma_5 f)$, derived through integration by parts and application of the equations of motion. This formulation naturally leads to the normalization factor $\frac{m_f}{f_a}$. In contrast, the scalar interactions (CP-even) explicitly break the shift symmetry. The scalar interactions in the unbroken phase of the SM can be described by the dimension-five operator $a H \bar{\psi}_{f,L(R)} \psi_{f,R(L)}$, which justifies the normalization factor $\frac{m_f}{f_a}$.

Note that the ALP-fermion interactions in Eq. (2.1) are proportional to the fermion mass m_f . Since the top quark mass m_t is significantly larger than the masses of all other fermions in the SM, we adopt the following simplified form of the Lagrangian in subsequent analysis:

$$\begin{aligned}\mathcal{L}^a &= -\frac{m_t}{f_a} c_t a \bar{\psi}_t \psi_t - i \frac{m_t}{f_a} \tilde{c}_t a \bar{\psi}_t \gamma_5 \psi_t \\ &= -\frac{m_t}{f_a} a \bar{\psi}_t (c_t + i \gamma_5 \tilde{c}_t) \psi_t .\end{aligned}\tag{2.2}$$

Similar to the Higgs-top coupling in the SM, the ALP-top coupling, as evident from Eq. (2.2), is also proportional to m_t . Due to the large mass of top quark, the Higgs exhibits a top-philic nature. Several studies (e.g., Refs. [51, 54]) have explored generic CP-even or CP-odd top-philic scalars, deriving constraints on their couplings with the top quark. A phenomenology of top-philic ALPs is discussed in Refs. [55, 56].

3 The Chromoelectromagnetic Dipole Moment

Similar to how photon-fermion interactions are described by a Lagrangian incorporating the effective electromagnetic dipole moment (EMDM), the dynamics of quark-antiquark pairs and their interactions with gluons can be characterized by a Lagrangian that includes the effective chromoelectromagnetic dipole moment (CEMDM). The effective Lagrangian incorporating the quark CEMDM, quark EDM, and the Weinberg operator can be expressed as [36, 57–62]:

$$\begin{aligned}\mathcal{L}_{\text{eff}} &= -\frac{1}{2} \bar{\psi}_{q,A} \sigma^{\mu\nu} (\mu_q^C + i \gamma_5 d_q^C) \psi_{q,B} G_{\mu\nu}^a T_{AB}^a \\ &\quad -\frac{1}{2} \bar{\psi}_q \sigma^{\mu\nu} (\mu_q^E + i \gamma_5 d_q^E) \psi_q F_{\mu\nu} \\ &\quad -\frac{1}{6} \mathcal{W} f^{abc} \epsilon^{\mu\nu\rho\sigma} G_{\mu,\alpha}^a G_{\nu}^{b,\alpha} G_{\rho\sigma}^c .\end{aligned}\tag{3.1}$$

Here, $\sigma^{\mu\nu} = \frac{i}{2} [\gamma^\mu, \gamma^\nu]$, where γ^μ are the Dirac gamma matrices. In the first term, the CMDM, denoted by μ_q^C , represents the CP-conserving contribution, while the CEDM, d_q^C , corresponds to the CP-violating part. Similarly, in the second term, the magnetic dipole moment (MDM) and EDM are denoted by μ_q^E and d_q^E , respectively. The CP-violating Weinberg operator is represented by the third term, where \mathcal{W} denotes the Wilson coefficient. In this term, the antisymmetric Levi-Civita tensor $\epsilon^{\mu\nu\rho\sigma}$ introduces CP violation. The color generators of $SU(3)_C$ are given by T_{AB}^a , where A and B label the quark color indices, and a represents the gluon color index. The field strength tensors corresponding to the photon and the gluon are defined as follows:

$$\begin{aligned}F_{\mu\nu} &= \partial_\mu A_\nu - \partial_\nu A_\mu , \\ G_{\mu\nu}^a &= \partial_\mu g_\nu^a - \partial_\nu g_\mu^a - g_s f^{abc} g_{\mu,b} g_{\nu,c} ,\end{aligned}\tag{3.2}$$

where $g_s = \sqrt{4\pi\alpha_s}$ is the strong coupling constant and f^{abc} are the structure constants of $SU(3)_C$. In the SM, CMDM arises at the one-loop level [63–65], whereas the CEDM

emerges only at three-loop order [66], making it significantly suppressed. In standard conventions, the EMDM and CEMDM are typically expressed in dimensionless form as follows [59, 61, 62, 67]:

$$\begin{aligned}\hat{\mu}_q^E &= \left(\frac{m_q}{e}\right) \mu_q^E, & \hat{d}_q^E &= \left(\frac{m_q}{e}\right) d_q^E, \\ \hat{\mu}_q^C &= \left(\frac{m_q}{g_s}\right) \mu_q^C, & \hat{d}_q^C &= \left(\frac{m_q}{g_s}\right) d_q^C,\end{aligned}\quad (3.3)$$

where m_q is the mass of quark. The CEMDM can develop absorptive contributions, especially in regimes where the momentum transfer becomes timelike ($q^2 > 0$). This is particularly evident in top-quark pair production ($t\bar{t}$) in pp collisions [61, 62].

Based on Eq. (3.1), we can express the effective vertex responsible for generating the EMDM and CEMDM in the following way:

$$\begin{aligned}\Gamma_E^\mu &= \sigma^{\mu\nu} q_\nu (\mu_q^E + i\gamma_5 d_q^E), \\ \Gamma_C^\mu &= \sigma^{\mu\nu} q_\nu (\mu_q^C + i\gamma_5 d_q^C) T_{AB}^a,\end{aligned}\quad (3.4)$$

where q_ν is the photon (gluon) momentum transfer for the vertex $\Gamma_{E(C)}^\mu$. One can write the corresponding invariant amplitude as follows:

$$\mathcal{M}_{E(C)} = \mathcal{M}_{E(C)}^\mu \epsilon_\mu^{E(C)}(\vec{q}), \quad (3.5)$$

where p and p' are the momenta of the external quarks, with $q = p' - p$. The Lorentz structure can be written as:

$$\mathcal{M}_{E(C)}^\mu = \bar{u}(p') \Gamma_{E(C)}^\mu u(p). \quad (3.6)$$

4 Calculation of the Top Quark CEDM

In this section, we discuss the one-loop and two-loop computations of the top quark CEDM induced by the ALP. Note that in the following calculations, we take the external gluon to be off-shell.

4.1 One-loop contribution

Fig. 1 shows the diagram contributing to the top quark CEDM at one-loop level. The ALP propagator is depicted as a red line, while ALP-top quark interaction vertices are marked by blue dots.

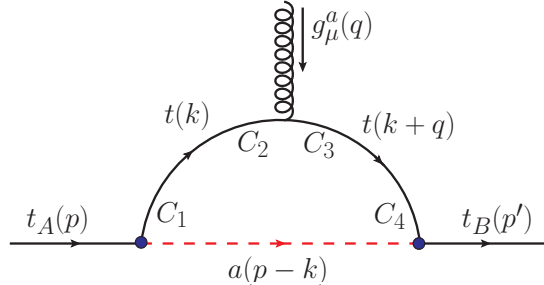


Figure 1. One-loop contributions to the top quark CEDM induced by the ALP. The ALP propagator is shown as a red line, with ALP-top quark interaction vertices indicated by blue dots.

The one-loop amplitude associated with the diagram in Fig. 1 takes the form:

$$\begin{aligned} \mathcal{M}_{1L}^\mu = & \int \frac{d^d k}{(2\pi)^d} \bar{u}(p') \left[\{-iy_{att}(c_t + i\gamma_5 \tilde{c}_t) \delta_{C_4 B}\} \left\{ \frac{i(\not{k} + \not{q} + m_t)}{(k+q)^2 - m_t^2} \delta_{C_3 C_4} \right\} (-ig_s T_{C_2 C_3}^a \gamma^\mu) \right. \\ & \times \left. \left\{ \frac{i(\not{k} + m_t)}{k^2 - m_t^2} \delta_{C_1 C_2} \right\} \{-iy_{att}(c_t + i\gamma_5 \tilde{c}_t) \delta_{AC_1}\} \left\{ \frac{i}{(p-k)^2 - m_a^2} \right\} \right] u(p), \end{aligned} \quad (4.1)$$

where $y_{att} = \frac{m_t}{f_a}$. After evaluating the loop integral, we extract the coefficient of $\gamma_5 \sigma^{\mu\nu} q_\nu$ to obtain the CEDM. Using Eq. (3.3), the top quark CEDM can then be expressed as:

$$\begin{aligned} \hat{d}_t^C(q^2)|_{1L} = & \frac{4y_{att}^2 m_t^2}{(4\pi)^2} c_t \tilde{c}_t \left[\frac{1}{4m_t^2 - q^2} \left\{ f_1[m_t^2, m_t, m_a] - f_1[q^2, m_t, m_t] \right. \right. \\ & \left. \left. + \frac{1}{2} \left(\frac{m_a^2}{m_t^2} \right) \log \left(\frac{m_a^2}{m_t^2} \right) - m_a^2 f_2[m_t^2, m_t^2, q^2, m_t, m_a, m_t] \right\} \right], \end{aligned} \quad (4.2)$$

where the generic forms of the functions $f_1[m_1, m_2, m_3]$ and $f_2[s_1, s_2, s_3, m_1, m_2, m_3]$ are defined in Appendix A. We can easily evaluate the top quark CEDM at $q^2 = 0$ as follows:

$$\hat{d}_t^C(0)|_{1L} = \frac{2y_{att}^2}{(4\pi)^2} c_t \tilde{c}_t \left[1 + \left(\frac{2m_t^2 - m_a^2}{4m_t^2 - m_a^2} \right) f_1[m_t^2, m_t, m_a] + \frac{1}{2} \left(\frac{m_a^2}{m_t^2} \right) \log \left(\frac{m_t^2}{m_a^2} \right) \right]. \quad (4.3)$$

4.2 Two-loop contribution

This section details the computation of the two-loop Barr-Zee-type contributions to the top quark CEDM. The relevant Feynman diagram, including momentum assignments, is shown in Fig. 2, with color coding consistent with Fig. 1. The calculation follows the methodology described in Refs. [68–70].

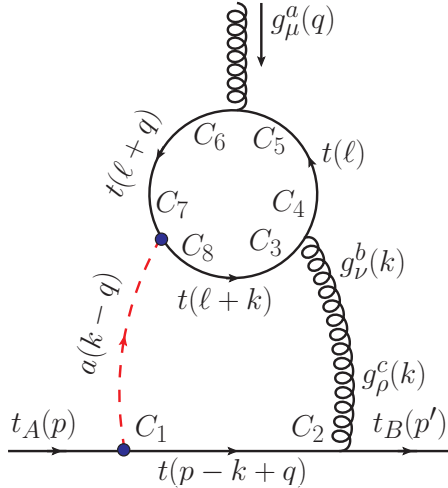


Figure 2. Two-loop contributions to the top quark CEDM induced by the ALP. The color coding is the same as in Fig. 1.

The complete two-loop amplitude corresponding to the diagram in Fig. 2 can be expressed as follows:

$$\begin{aligned}
\mathcal{M}_{2L}^\mu = & \int \frac{d^d k}{(2\pi)^d} \int \frac{d^d \ell}{(2\pi)^d} \bar{u}(p') \left[(-ig_s T_{C_2 B}^c \gamma^\rho) \left\{ \frac{i(\not{p} - \not{k} + \not{q} + m_t)}{(p-k+q)^2 - m_t^2} \delta_{C_1 C_2} \right\} \{-iy_{att} \right. \\
& \times (c_t + i\gamma_5 \tilde{c}_t) \delta_{C_1 A}\} \left\{ \frac{i}{(k-q)^2 - m_a^2} \right\} \left\{ -\text{Tr} \left[(-ig_s T_{C_5 C_6}^a \gamma^\mu) \left\{ \frac{i(\not{\ell} + m_t)}{\ell^2 - m_t^2} \right. \right. \right. \\
& \times \delta_{C_4 C_5} \left\{ (-ig_s T_{C_3 C_4}^b \gamma^\nu) \left\{ \frac{i(\not{\ell} + \not{k} + m_t)}{(\ell+k)^2 - m_t^2} \delta_{C_8 C_3} \right\} \{-iy_{att}(c_t + i\gamma_5 \tilde{c}_t) \delta_{C_7 C_8}\} \right. \\
& \left. \left. \left. \times \left\{ \frac{i(\not{\ell} + \not{q} + m_t)}{(\ell+q)^2 - m_t^2} \delta_{C_6 C_7} \right\} \right] \right\} \left(\frac{-ig_{\nu\rho}}{k^2} \delta_{bc} \right) \right] u(p) . \quad (4.4)
\end{aligned}$$

We can reformulate Eq. (4.4) in the following form:

$$\mathcal{M}_{2L}^\mu = \mathcal{K}_1 \int \frac{d^d k}{(2\pi)^d} \bar{u}(p') \left[\left\{ \frac{\gamma_\nu (\not{p} - \not{k} + \not{q} + m_t)(c_t + i\gamma_5 \tilde{c}_t)}{\mathcal{D}_1 \mathcal{D}_2 \mathcal{D}_3} \right\} [\Sigma^{\mu\nu}(k)] \right] u(p) , \quad (4.5)$$

where $\mathcal{K}_1 = -iy_{att} g_s T_{C_2 B}^c \delta_{C_1 C_2} \delta_{C_1 A} \delta_{bc} = -iy_{att} g_s T_{AB}^b$ and $\mathcal{D}_1 = k^2$, $\mathcal{D}_2 = (k-q)^2 - m_a^2$, and $\mathcal{D}_3 = (p-k+q)^2 - m_t^2$. The quantity $\Sigma^{\mu\nu}(k)$ can be expressed as follows:

$$\Sigma^{\mu\nu}(k) = \mathcal{K}_2 \int \frac{d^d \ell}{(2\pi)^d} \left[\frac{\text{Tr}[\gamma^\mu (\not{\ell} + m_t) \gamma^\nu (\not{\ell} + \not{k} + m_t) (c_t + i\gamma_5 \tilde{c}_t) (\not{\ell} + \not{q} + m_t)]}{\mathcal{D}_4 \mathcal{D}_5 \mathcal{D}_6} \right] , \quad (4.6)$$

where $\mathcal{K}_2 = -y_{att} g_s^2 T_{C_5 C_6}^a \delta_{C_4 C_5} T_{C_3 C_4}^b \delta_{C_8 C_3} \delta_{C_7 C_8} \delta_{C_6 C_7} = -\frac{1}{2} y_{att} g_s^2 \delta_{ab}$ (using $\text{Tr}[T^a T^b] = \frac{1}{2} \delta^{ab}$) and $\mathcal{D}_4 = \ell^2 - m_t^2$, $\mathcal{D}_5 = (\ell+k)^2 - m_t^2$, and $\mathcal{D}_6 = (\ell+q)^2 - m_t^2$. First, we evaluate the integral $\Sigma^{\mu\nu}(k)$ over the loop momentum variable “ ℓ ”. After that, this “ k ”-dependent result is then used to compute the second loop integral in Eq. (4.5). Using Feynman parameterization, we can express Eq. (4.6) in the following form:

$$\begin{aligned}
\Sigma^{\mu\nu}(k) = & \mathcal{K}_2 \left[\mathcal{G}_1(k) g^{\mu\nu} + \mathcal{G}_2(k) k^\mu q^\nu + \mathcal{G}_3(k) k^\nu q^\mu + \mathcal{G}_4(k) k^\mu k^\nu \right. \\
& \left. + \mathcal{G}_5(k) q^\mu q^\nu + \mathcal{G}_6(k) \epsilon^{\mu\nu\rho\sigma} k_\rho q_\sigma \right] . \quad (4.7)
\end{aligned}$$

The loop-momentum-dependent functions $\mathcal{G}_1(k), \dots, \mathcal{G}_6(k)$ are given by:

$$\begin{aligned}
\mathcal{G}_1(k) = & \frac{i}{(4\pi)^2} \int_0^1 dx \int_0^{1-x} dy \, 4c_t m_t \left[1 - \frac{m_t^2}{\Delta(k, x, y)} + \frac{y^2 k^2 + (2xy - 1)(k \cdot q) + x^2 q^2}{\Delta(k, x, y)} \right] , \\
\mathcal{G}_2(k) = & \frac{i}{(4\pi)^2} \int_0^1 dx \int_0^{1-x} dy \, 4c_t m_t \left[\frac{1 - 4xy}{\Delta(k, x, y)} \right] , \\
\mathcal{G}_3(k) = & \frac{i}{(4\pi)^2} \int_0^1 dx \int_0^{1-x} dy \, 4c_t m_t \left[-\frac{(1-2x)(1-2y)}{\Delta(k, x, y)} \right] ,
\end{aligned}$$

$$\begin{aligned}
\mathcal{G}_4(k) &= \frac{i}{(4\pi)^2} \int_0^1 dx \int_0^{1-x} dy \, 8c_t m_t \left[\frac{y(1-2y)}{\Delta(k, x, y)} \right], \\
\mathcal{G}_5(k) &= \frac{i}{(4\pi)^2} \int_0^1 dx \int_0^{1-x} dy \, 8c_t m_t \left[\frac{x(1-2x)}{\Delta(k, x, y)} \right], \\
\mathcal{G}_6(k) &= \frac{i}{(4\pi)^2} \int_0^1 dx \int_0^{1-x} dy \, 4\tilde{c}_t m_t \left[\frac{1}{\Delta(k, x, y)} \right],
\end{aligned} \tag{4.8}$$

where $\Delta(k, x, y) = x(x-1)q^2 + y(y-1)k^2 + 2xy(k \cdot q) + m_t^2$, x and y represent the Feynman parameters. By substituting the expressions for $\mathcal{G}_1(k)$, \dots , $\mathcal{G}_6(k)$ from Eq. (4.8), we evaluate the loop momentum integral in Eq. (4.5) over the variable “ k ”. This yields six different integrals, each associated with one of the functions defined in Eq. (4.8). We then isolate the coefficient of $\gamma_5 \sigma^{\mu\nu} q_\nu$ to extract the two-loop form factors contributing to the CEDM of the top quark. Note that the terms involving $\mathcal{G}_3(k)$ and $\mathcal{G}_5(k)$ do not contribute to this coefficient, as it vanishes in both cases. Moreover, the form factor associated with $\mathcal{G}_4(k)$ also evaluates to zero. Thus, the only non-zero two-loop form factors are $\mathcal{F}_1(q^2)$, $\mathcal{F}_2(q^2)$, and $\mathcal{F}_6(q^2)$. Consequently, the CEDM of the top quark for $q^2 \neq 0$ can be expressed as follows:

$$\begin{aligned}
\hat{d}_t^C(q^2)|_{2L} &= \left(\frac{m_t}{g_s} \right) d_t^C(q^2)|_{2L} \\
&= \left(\frac{m_t}{g_s} \right) [\mathcal{F}_1(q)^2 + \mathcal{F}_2(q)^2 + \mathcal{F}_6(q)^2],
\end{aligned} \tag{4.9}$$

where the complete analytical expressions for the form factors $\mathcal{F}_1(q^2)$, $\mathcal{F}_2(q^2)$, and $\mathcal{F}_6(q^2)$ are provided in Appendix A.

Finally, the total CEDM (one-loop + two-loop) of the top quark is given by:

$$\hat{d}_t^C(q^2) = \hat{d}_t^C(q^2)|_{1L} + \hat{d}_t^C(q^2)|_{2L}. \tag{4.10}$$

5 Contribution to the Weinberg Operator, Neutron EDM, and Mercury EDM

The QCD renormalization group (RG) evolution causes the operators in Eq. (3.1) to run and mix. These effects have been calculated up to next-to-leading logarithmic (NLL) precision [71]. Specifically, the Weinberg operator induces mixing into quark EDMs and CEDMs but the reverse does not occur. However, it has long been established that quark CEDMs generate a finite threshold correction to the Weinberg operator upon integrating out a heavy quark (top) [72, 73].

Figs. 3a and 3b depict the diagrams contributing to the Weinberg operator \mathcal{W} at the top quark threshold, where the red blob denotes the insertion of the CEDM of the top quark.

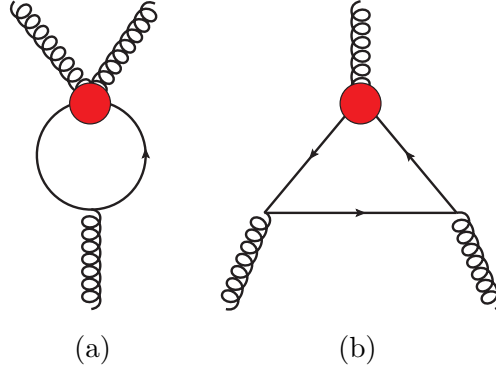


Figure 3. Figures (a) and (b) show the diagrams contributing to the Weinberg operator at the top quark threshold, with the red blob representing the CEDM insertion.

One can write the threshold correction to \mathcal{W} as [60]:

$$\delta\mathcal{W}^{(t)} = \frac{g_s^2}{32\pi^2 m_t} d_t^C(m_t) , \quad (5.1)$$

where $d_t^C(m_t)$ can be found from Eq. (4.9). The finite correction in \mathcal{W} , along with the subsequent RG running down to hadronic energies, results in non-zero contributions to both the EDMs and CEDMs of light quarks. Following Ref. [60], which performs the RG running of the Weinberg operator at NLL accuracy down to the hadronic scale, $\mu_{\text{Had}} \sim 1$ GeV, we can write $d_{u,d}^E(\mu_{\text{Had}})$, $d_{u,d}^C(\mu_{\text{Had}})$, and $\mathcal{W}(\mu_{\text{Had}})$ in terms of $d_t^C(m_t)$ as follows:

$$\begin{aligned} d_u^E &= -3.1 \times 10^{-9} e \left(\frac{d_t^C(m_t)}{g_s} \right) , \\ d_d^E &= 3.5 \times 10^{-9} e \left(\frac{d_t^C(m_t)}{g_s} \right) , \\ d_u^C &= 8.9 \times 10^{-9} d_t^C(m_t) , \\ d_d^C &= 2.0 \times 10^{-8} d_t^C(m_t) , \\ \mathcal{W} &= 1.0 \times 10^{-5} \text{ GeV}^{-1} \left(\frac{d_t^C(m_t)}{g_s} \right) , \end{aligned} \quad (5.2)$$

where $m_t = 173.3$ GeV, $m_d^{\overline{\text{MS}}}(2 \text{ GeV}) = (4.7 \pm 0.1)$ MeV, $m_u^{\overline{\text{MS}}}(2 \text{ GeV}) = (2.1 \pm 0.1)$ MeV, and $\alpha_s^{\overline{\text{MS}}}(m_Z) = 0.118$ have been used. Note that using Eq. (4.10), we obtain an exact calculation of $d_t^C(m_t)$ by fixing the momentum transfer at $q^2 = m_t^2$. Finally, using Eq. (5.2), we can compute the EDM of neutron and mercury (Hg). The present experimental constraints on the EDM of neutron and Hg are:

$$\begin{aligned} |d_n^E|_{\text{Exp.}} &< 1.8 \times 10^{-26} e \text{ cm (90\% C.L.) [74]}, \\ |d_{\text{Hg}}^E|_{\text{Exp.}} &< 7.4 \times 10^{-30} e \text{ cm (95\% C.L.) [75]}. \end{aligned} \quad (5.3)$$

Following the approach in Ref. [76], we may write the contributions to the neutron and Hg EDMs as follows [50, 60, 77]:

$$\begin{aligned} d_n^E &= (1 \pm 0.5) \left[1.1e \left(\frac{d_d^C}{g_s} + 0.5 \frac{d_u^C}{g_s} \right) + 1.4(d_d^E - 0.25d_u^E) \right] + (22 \pm 10) \times 10^{-3} \text{ GeV } e \mathcal{W} , \\ d_{\text{Hg}}^E &= -1.8 \times 10^{-4} \text{ GeV}^{-1} e \bar{g}_{\pi NN}^{(1)} , \end{aligned} \quad (5.4)$$

where $\bar{g}_{\pi NN}^{(1)} = 4_{-2}^{+8}(d_u^C - d_d^C) \text{ GeV}$. All quantities are calculated at the energy scale of $\mu_{\text{Had}} \sim 1 \text{ GeV}$. Note that the numerical values and associated uncertainties for the relevant matrix elements, including the Weinberg operator's contribution to the d_n^E , have been computed using QCD sum rule [78].

6 Constraints on ALP-Top Quark Coupling from Other Searches

The study in Ref. [79] explored the coupling of a light ALP to top quarks, considering both direct and indirect probes. The direct search focused on $t\bar{t}$ production associated with an ALP, while the indirect approach investigated ALP production via the gluon fusion process, followed by decays into top pairs. The limit at 95% C.L. obtained from the ATLAS search is given by

$$\left| \frac{c_t}{f_a} \right| < 1.81 \times 10^{-3} \text{ GeV}^{-1} . \quad (6.1)$$

The production of di-boson, mediated by an ALP through its coupling with the top quark leads to the following constraint

$$\left| \frac{c_t}{f_a} \right| < 4.44 \times 10^{-2} \text{ GeV}^{-1} . \quad (6.2)$$

The study of $t\bar{t}$ production involving a high- p_T top quark, as measured by ATLAS, was used in Ref. [79] to derive the constraint

$$\left| \frac{c_t}{f_a} \right| < 5.90 \times 10^{-3} \text{ GeV}^{-1} . \quad (6.3)$$

In Ref. [80], the study builds upon the work of Ref. [81] by calculating the limits on the ALP- WW and ALP- $Z\gamma$ couplings using ATLAS non-resonant searches in the WW and $Z\gamma$ final states. Ref [79] studied the $Z\gamma$ final state and derived the following 95% C.L. limit (for $m_a < 100 \text{ GeV}$):

$$\left| \frac{c_t}{f_a} \right| < 9.09 \times 10^{-2} \text{ GeV}^{-1} . \quad (6.4)$$

Constraints on the ALP- ZZ coupling are further studied in Ref. [82] through a CMS non-resonant searches of ZZ production. This leads to the constraint on ALP-top coupling at 95% C.L. as follows:

$$\left| \frac{c_t}{f_a} \right| < 5.88 \times 10^{-2} \text{ GeV}^{-1} . \quad (6.5)$$

Based on the low-energy precision measurements of rare Kaon [83] and B -meson decays [84] from the NA62 and BABAR collaboration, Ref. [79] derived the following limits:

$$\left| \frac{c_t}{f_a} \right| < 2.80 \times 10^{-4} \text{ GeV}^{-1} \quad (K \text{ decays: } m_a < 110 \text{ MeV and } m_a \in [160, 260] \text{ MeV}) , \quad (6.6)$$

$$\left| \frac{c_t}{f_a} \right| < 1.15 \times 10^{-6} \text{ GeV}^{-1} \quad (B \text{ decays: } m_a \lesssim 5 \text{ GeV}) . \quad (6.7)$$

Ref. [85] provides a comprehensive study of ALPs in top-pair production at the LHC, deriving constraints on the ALP-top coupling from the total cross section and differential distributions. The resulting bound is given by:

$$\left| \frac{c_t}{f_a} \right| < 7 \times 10^{-3} \text{ GeV}^{-1} , \quad (\text{for } 0 < m_a < 200 \text{ GeV}). \quad (6.8)$$

Based on the measurements of top-antitop production accompanied by di-muon resonances from the ATLAS [86] and CMS [87] experiments, the following constraint is derived:

$$\left| \frac{c_t}{f_a} \right| < 1 \times 10^{-3} \text{ GeV}^{-1} , \quad (\text{LHC } 150 \text{ fb}^{-1}). \quad (6.9)$$

An analysis of top quark pair production at the LHC yields the bound [88]:

$$\left| \frac{c_t}{f_a} \right| < 4 \times 10^{-3} \text{ GeV}^{-1} , \quad (\text{for } m_a = 300 \text{ GeV}). \quad (6.10)$$

A related study in Ref. [55] finds a slightly weaker limit:

$$\left| \frac{c_t}{f_a} \right| < 6 \times 10^{-3} \text{ GeV}^{-1} , \quad (10 \text{ GeV} < m_a < 200 \text{ GeV}). \quad (6.11)$$

7 Constraints on ALP-Top Coupling from Top Quark CEDM, Neutron EDM, and Mercury EDM

In Sec. 4 and 5, we have already discussed the relevant formulae for computing the CEDM and EDMs. In this section, we present the numerical values of the constraints on the ALP-top coupling derived from the top quark CEDM, the neutron EDM, and the mercury EDM. The top quark CEDM, evaluated up to two-loop order at $q^2 = m_t^2$, is subsequently used to compute the corresponding contributions to the EDMs of the neutron and mercury. We provide the resulting bounds on the ALP-top coupling for various values of the ALP mass, m_a , as obtained from each observable.

In our scenario, it is important to note that the CEDM of the top quark, and consequently the EDM of the neutron and mercury, develops an absorptive part for $q^2 > 0$. Specifically, it contains both real and imaginary components.

Constraints from CEDM of top quark: In Fig. 4, we show the variation of $\hat{d}_t^C / \left(\frac{c_t \tilde{c}_t}{f_a^2} \right)$ with the ALP mass, which is varied over the range $m_a \in [5, 100] \text{ GeV}$. As an example, for $m_a = 5 \text{ GeV}$, we have:

$$\left| \hat{d}_t^C(m_t) \right| = 422 \times \left(\frac{c_t \tilde{c}_t}{f_a^2} \right) . \quad (7.1)$$

Applying the latest experimental bound on the top quark CEDM given in Eq. (1.1), we obtain from Eq. (7.1):

$$\frac{c_t}{f_a} \cdot \frac{\tilde{c}_t}{f_a} < 7.11 \times 10^{-5} \text{ GeV}^{-2} . \quad (7.2)$$

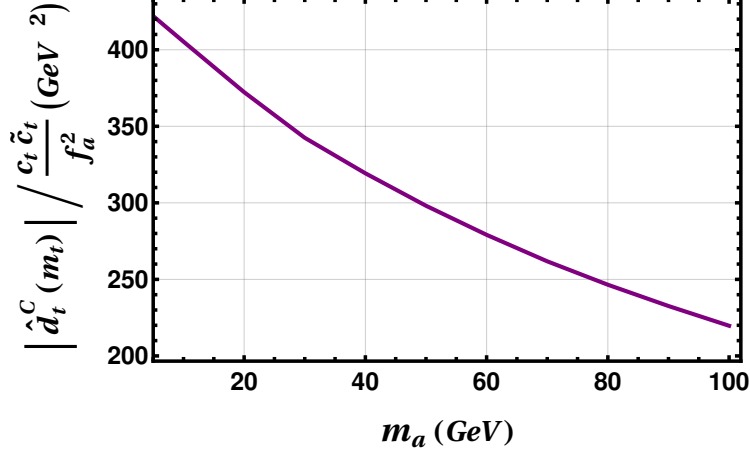


Figure 4. Variation of the CEDM of the top quark in unit of $\frac{c_t \tilde{c}_t}{f_a^2}$ with the ALP mass m_a .

In the case of maximal CP violation, where $c_t \simeq \tilde{c}_t$, we obtain:

$$\left| \frac{c_t}{f_a} \right| < 8.43 \times 10^{-3} \text{ GeV}^{-1} \implies \left| \frac{f_a}{c_t} \right| > 119 \text{ GeV} . \quad (7.3)$$

Similarly, we can derive the limit for $m_a = 100 \text{ GeV}$ as:

$$\left| \hat{d}_t^C(m_t) \right| = 220 \times \left(\frac{c_t \tilde{c}_t}{f_a^2} \right) . \quad (7.4)$$

Therefore, we obtain:

$$\left| \frac{c_t}{f_a} \right| < 1.17 \times 10^{-2} \text{ GeV}^{-1} \implies \left| \frac{f_a}{c_t} \right| > 86 \text{ GeV} . \quad (7.5)$$

Thus, the constraint derived from the top quark CEDM is found to be more stringent than those from di-boson production, ATLAS non-resonant searches in the $Z\gamma$ final state, and CMS non-resonant ZZ production searches. In fact, the limit from top quark CEDM is nearly an order of magnitude stronger than the bounds set by the ATLAS $Z\gamma$ and CMS ZZ non-resonant searches.

Constraints from EDM of neutron: Using Eq. (5.4), we calculate the neutron EDM for an ALP mass of $m_a = 5 \text{ GeV}$ as:

$$\left| d_n^E \right| = 1.78 \times 10^{-20} \times \left(\frac{c_t \tilde{c}_t}{f_a^2} \right) e \text{ cm} . \quad (7.6)$$

Using the experimental limit on $|d_n^E|$ given in Eq. (5.3), we obtain:

$$\frac{c_t}{f_a} \cdot \frac{\tilde{c}_t}{f_a} < 1.01 \times 10^{-6} \text{ GeV}^{-2} . \quad (7.7)$$

With $c_t \simeq \tilde{c}_t$, this gives:

$$\left| \frac{c_t}{f_a} \right| < 1 \times 10^{-3} \text{ GeV}^{-1} \implies \left| \frac{f_a}{c_t} \right| > 1000 \text{ GeV} . \quad (7.8)$$

In the same way, the limit for $m_a = 100 \text{ GeV}$ can be obtained as follows:

$$|d_n^E| = 9.30 \times 10^{-21} \times \left(\frac{c_t \tilde{c}_t}{f_a^2} \right) e \text{ cm} . \quad (7.9)$$

Therefore,

$$\left| \frac{c_t}{f_a} \right| < 1.39 \times 10^{-3} \text{ GeV}^{-1} \implies \left| \frac{f_a}{c_t} \right| > 719 \text{ GeV} . \quad (7.10)$$

Thus, the constraint on the ALP-top coupling derived from the neutron EDM is nearly an order of magnitude tighter than that from the top quark CEDM. Moreover, it surpasses bounds derived from ATLAS searches for $t\bar{t}$ production associated with an ALP, high- p_T top quark measurements, and LHC analyses of total cross-sections and differential distributions in $t\bar{t}$ production. In particular, the limit from neutron EDM is about twice as strong as the ATLAS $t\bar{t}a$ search and nearly six times stronger than the high- p_T $t\bar{t}$ measurement.

Constraints from EDM of mercury: We employ Eq. (5.4) to evaluate the mercury EDM. For $m_a = 5 \text{ GeV}$, we obtain:

$$|d_{\text{Hg}}^E| = 1.16 \times 10^{-24} \times \left(\frac{c_t \tilde{c}_t}{f_a^2} \right) e \text{ cm} . \quad (7.11)$$

From the experimental constraint on $|d_{\text{Hg}}^E|$ as noted in Eq. (5.3), we obtain:

$$\frac{c_t}{f_a} \cdot \frac{\tilde{c}_t}{f_a} < 6.38 \times 10^{-6} \text{ GeV}^{-2} . \quad (7.12)$$

For $c_t \simeq \tilde{c}_t$, this yields:

$$\left| \frac{c_t}{f_a} \right| < 2.52 \times 10^{-3} \text{ GeV}^{-1} \implies \left| \frac{f_a}{c_t} \right| > 397 \text{ GeV} . \quad (7.13)$$

Similarly, for $m_a = 100 \text{ GeV}$, we obtain:

$$|d_{\text{Hg}}^E| = 6.04 \times 10^{-25} \times \left(\frac{c_t \tilde{c}_t}{f_a^2} \right) e \text{ cm} . \quad (7.14)$$

Therefore, we obtain the following limit:

$$\left| \frac{c_t}{f_a} \right| < 3.50 \times 10^{-3} \text{ GeV}^{-1} \implies \left| \frac{f_a}{c_t} \right| > 286 \text{ GeV} . \quad (7.15)$$

Thus, the constraint on the ALP-top coupling obtained from the mercury EDM is over three times stronger than that from the top quark CEDM but remains significantly weaker than the bound derived from the neutron EDM.

8 Summary and Conclusions

In this work, we consider an ALP that arises as a mixture of scalar and pseudoscalar operators. Due to this mixed nature, the ALP induces CP violation when it couples to the SM fermions. Such CP violation can generate EDMs for quarks and leptons and CEDMs for quarks. We compute the CEDM of the top quark mediated by this ALP at one-loop and two-loop levels, where the two-loop contribution stems from the Barr-Zee-type diagrams. A key distinction is that, unlike the static EDMs of fermions, which are constrained by low-energy precision experiments, the CEDM can only be probed dynamically in high-energy collisions. To retain generality, we consider the external gluon to be off-shell, i.e., $q^2 \neq 0$, and ultimately evaluate the CEDM at $q^2 = m_t^2$, corresponding to the pole mass of the top quark. Since the top quark CEDM can induce finite threshold corrections to the Weinberg operator upon integrating out the top quark, we have computed its contribution to the Weinberg operator explicitly. This finite correction, combined with the subsequent RG running down to the hadronic scale, generates non-zero contributions to both the EDMs and CEDMs of light quarks. We then express the EDMs and CEDMs of light quarks at the hadronic scale in terms of the top quark CEDM evaluated at its pole mass. These results are subsequently used to calculate the EDMs of the neutron and mercury. Using the current experimental upper limits on the top quark CEDM and the EDMs of the neutron and mercury, we derive bounds on the ALP-top coupling. Our analysis shows that the constraint derived from the neutron EDM is significantly more stringent than those from the top quark CEDM and the mercury EDM. From the neutron EDM constraint, we obtain a bound on the ALP-top coupling: $\left| \frac{c_t}{f_a} \right| < 1 \times 10^{-3} \text{ GeV}^{-1}$ for an ALP mass of $m_a = 5 \text{ GeV}$. Thus, our bound on the ALP-top coupling, $\left| \frac{c_t}{f_a} \right|$, is approximately twice as strong as the limit derived from the ATLAS $t\bar{t}a$ search and about six times stronger than the ATLAS measurement of high- p_T $t\bar{t}$ production.

9 Acknowledgements

I would like to thank U. Chattopadhyay for carefully reading the manuscript and for the valuable discussions. I also thank D. Das for helpful discussions.

Appendix

A Two-Loop Form Factors

The two-loop form factors contributing to the CEDM of the top quark, as used in Eq. (4.9), can be expressed as follows:

$$\begin{aligned} \mathcal{F}_1(q^2) = & -\frac{2y_{att}^2 g_s^3 m_t}{(4\pi)^4} c_t \tilde{c}_t \int_0^1 dx \int_0^{1-x} dy \left[\frac{8m_t^2 f_1[m_t^2, m_t, m_a]}{q^2(q^2 - 4m_t^2)} + \frac{4(m_a^2 - q^2)}{q^2(q^2 - 4m_t^2)} \log \left(\frac{m_t^2}{m_a^2 - q^2} \right) \right] \\ & - \frac{4 \{ -m_a^2 q^2 + 2m_t^2(m_a^2 + q^2) \} f_2[m_t^2, m_t^2, q^2, m_a, m_t, 0]}{q^2(q^2 - 4m_t^2)} - \frac{2m_t^2}{M^2 + \xi \{ m_a^2 - q^2(1 + \xi) \}} \end{aligned}$$

$$\begin{aligned}
& \times \left\{ -\frac{2q^2(1+\xi)^3 f_1[q^2(1+\xi)^2, M, m_a]}{\Lambda[m_t^2, q^2(1+\xi)^2, m_t^2 + q^2\xi(1+\xi)]} - \frac{(-M^2 + m_a^2 + q^2(-1+\xi^2)) \log\left(\frac{M^2}{m_a^2}\right)}{q^2(q^2 - 4m_t^2)(1+\xi)} \right. \\
& + \frac{2(-m_a^2 + q^2) \log\left(\frac{m_a^2}{m_a^2 - q^2}\right)}{q^2(q^2 - 4m_t^2)} + \frac{2\xi(-M^2 + q^2\xi^2) \log\left(\frac{M^2}{M^2 - q^2\xi^2}\right)}{\Lambda[m_t^2, q^2\xi^2, m_t^2 + q^2\xi(1+\xi)]} \\
& + \frac{2\{-m_a^2 q^2 + 2m_t^2(m_a^2 + q^2)\} f_2[m_t^2, m_t^2, q^2, m_a, m_t, 0]}{q^2(q^2 - 4m_t^2)} \\
& + \frac{2\xi^2\{q^2(M^2 - q^2\xi(1+\xi)) + m_t^2(-2M^2 + 2q^2\xi(2+\xi))\}}{\Lambda[m_t^2, q^2\xi^2, m_t^2 + q^2\xi(1+\xi)]} \\
& \times f_2[m_t^2, q^2\xi^2, m_t^2 + q^2\xi(1+\xi), m_t, 0, M] \\
& - \frac{2(1+\xi)^2\{-m_a^2 q^2(1+\xi) + 2m_t^2(-M^2 + m_a^2 + q^2(1+\xi)^2)\}}{\Lambda[m_t^2, q^2(1+\xi)^2, m_t^2 + q^2\xi(1+\xi)]} \\
& \times f_2[m_t^2, q^2(1+\xi)^2, m_t^2 + q^2\xi(1+\xi), m_t, m_a, M] \left\{ \frac{1}{y(y-1)} \right\} \\
& + \left\{ \frac{1}{y(y-1)} \right\} \left\{ \frac{4m_t^2(-1+2y^2+2yz)(1+\xi) f_1[m_t^2, m_t, m_a]}{\Lambda[m_t^2, q^2(1+\xi)^2, m_t^2 + q^2\xi(1+\xi)]} \right. \\
& + \frac{2q^2(1+\xi)^2 f_1[q^2(1+\xi)^2, M, m_a]}{(M^2 + \xi(m_a^2 - q^2(1+\xi))) \Lambda[m_t^2, q^2(1+\xi)^2, m_t^2 + q^2\xi(1+\xi)]} \\
& \times \left\{ M^2(1-2y^2-2yz) + m_a^2(-1+2yz-2y^2\xi) + q^2(1+\xi)(1-2z^2+2yz(-1+\xi) \right. \\
& \left. - \xi + 2y^2\xi) \right\} + \frac{2q^2(q^2 - 4m_t^2)\xi(1+\xi)(1-2xy+2y^2\xi)}{\Lambda[m_t^2, q^2\xi^2, m_t^2 + q^2\xi(1+\xi)] \Lambda[m_t^2, q^2(1+\xi)^2, m_t^2 + q^2\xi(1+\xi)]} \\
& \times \left\{ -2m_t^2 + q^2(1+\xi) \right\} f_1[m_t^2 + q^2\xi(1+\xi), m_t, M] \\
& - \frac{2m_t^2\{m_a^2(1-2y^2-2xy)\xi + M^2(1-2xy+2y^2\xi) + q^2\xi(1+\xi)(1-2xy+2y^2(1+\xi))\}}{q^2(q^2 - 4m_t^2)\xi(1+\xi)(m_t^2 + q^2\xi(1+\xi))} \\
& \times \log\left(\frac{m_t^2}{M^2}\right) + \frac{1}{(q^2 - 4m_t^2)\xi(m_t^2 + q^2\xi(1+\xi))} \log\left(\frac{m_t^2}{M^2}\right) \\
& \times \left\{ M^2(1-2xy+2y^2\xi) + \xi(2m_a^2(-1+2y^2+2xy)\xi - q^2(1+\xi)(-1+2xy+2y^2\xi)) \right\} \\
& + \frac{1}{q^2(q^2 - 4m_t^2)(1+\xi)^2(M^2 + \xi(m_a^2 - q^2(1+\xi)))} \left\{ M^4(-1+2y^2+2xy) \right. \\
& + q^4(1+\xi)^2(-1-2x^2(-1+\xi) - \xi^2 + 2y^2\xi(1+\xi) + 2xy(1+\xi^2)) - 2m_a^2 q^2(1+\xi) \\
& \times (-1+x^2 - \xi - \xi^2 + y^2\xi(2+3\xi) + 2xy(1+\xi+\xi^2)) + m_a^4(-1-2\xi-2\xi^2+2y^2\xi(1+2\xi) \\
& + 2xy(1+2\xi+2\xi^2)) + 2M^2(-q^2(1+\xi)(-x^2 - \xi + 2xy\xi + y^2(1+2\xi)) \\
& + m_a^2(-\xi + 2xy\xi + y^2(1+3\xi))) \left. \right\} \log\left(\frac{M^2}{m_a^2}\right) \\
& + \frac{2(-m_a^2 + q^2)\{m_a^2(1-2xy) + q^2(-1+2xy+2x^2)\}}{q^2(-4m_t^2 + q^2)(M^2 + \xi(m_a^2 - q^2(1+\xi)))} \log\left(\frac{m_a^2}{m_a^2 - q^2}\right) \\
& - \frac{2(M^2 - q^2\xi^2)\{M^2(2xy-1) + q^2\xi(2x^2 + \xi - 2xy\xi)\}}{(M^2 + \xi(m_a^2 - q^2(1+\xi))) \Lambda[m_t^2, q^2\xi^2, m_t^2 + q^2\xi(1+\xi)]} \log\left(\frac{M^2}{M^2 - q^2\xi^2}\right)
\end{aligned}$$

$$\begin{aligned}
& - \frac{2 \{2m_t^2 (m_a^2 + q^2) - m_a^2 q^2\} \{m_a^2 (2xy - 1) + q^2 (1 - 2xy - 2x^2)\} f_2 [m_t^2, m_t^2, q^2, m_a, m_t, 0]}{q^2 (q^2 - 4m_t^2) \{M^2 + \xi (m_a^2 - q^2(1 + \xi))\}} \\
& + \frac{2\xi \{M^2(1 - 2xy) + q^2\xi(-2x^2 - \xi + 2xy\xi)\}}{\{M^2 + \xi (m_a^2 - q^2(1 + \xi))\} \Lambda [m_t^2, q^2\xi^2, m_t^2 + q^2\xi(1 + \xi)]} \\
& \times \left\{ q^4\xi(1 + \xi) - M^2q^2 + 2m_t^2(M^2 - q^2\xi(2 + \xi)) \right\} f_2[m_t^2, q^2\xi^2, m_t^2 + q^2\xi(1 + \xi), m_t, 0, M] \\
& + \frac{M^2(1 - 2y^2 - 2xy) + m_a^2(2xy - 2y^2\xi - 1) + q^2(1 + \xi) \{1 - 2x^2 + 2xy(\xi - 1) - \xi + 2y^2\xi\}}{\{M^2 + \xi(m_a^2 - q^2(1 + \xi))\} \Lambda [m_t^2, q^2(1 + \xi)^2, m_t^2 + q^2\xi(1 + \xi)]} \\
& \times 2(1 + \xi) \left\{ 2m_t^2(m_a^2 - M^2 + q^2(1 + \xi)^2) - m_a^2q^2(1 + \xi) \right\} \\
& \times f_2[m_t^2, q^2(1 + \xi)^2, m_t^2 + q^2\xi(1 + \xi), m_t, m_a, M] \Bigg\} \quad (A.1)
\end{aligned}$$

$$\begin{aligned}
\mathcal{F}_2(q^2) = & - \frac{2y_{att}^2 g_s^3 m_t}{(4\pi)^4} c_t \tilde{c}_t \int_0^1 dx \int_0^{1-x} dy \left[\frac{1 - 4xy}{y(y - 1)} \right] \\
& \times \left[\frac{4m_a^2 q^4 (q^2 - 4m_t^2) (1 + \xi)^5 f_1 [q^2(1 + \xi)^2, M, m_a]}{\{M^2 + \xi(m_a^2 - q^2(1 + \xi))\} \Lambda [m_t^2, q^2(1 + \xi)^2, m_t^2 + q^2\xi(1 + \xi)]^2} \right. \\
& - \frac{2q^8 (q^2 - 4m_t^2)^3 \xi^3 (1 + \xi)^4 (1 + 2\xi) f_1 [m_t^2 + q^2\xi(1 + \xi), m_t, M]}{\Lambda [m_t^2, q^2\xi^2, m_t^2 + q^2\xi(1 + \xi)]^2 \Lambda [m_t^2, q^2(1 + \xi)^2, m_t^2 + q^2\xi(1 + \xi)]^2} \\
& + \frac{-4m_t^2\xi + M^2(1 + 2\xi) - q^2\xi(-1 + \xi + 2\xi^2)}{(4m_t^2 - q^2)\xi(m_t^2 + q^2\xi(1 + \xi))} \log \left(\frac{m_t^2}{m_a^2} \right) \\
& + \frac{M^4 q^2(1 + 3\xi + 2\xi^2) - M^2\xi \{2m_t^2(m_a^2 + 2q^2(1 + \xi)) + q^2(1 + \xi)(4q^2\xi(1 + \xi) - m_a^2)\}}{q^2(q^2 - 4m_t^2)\xi(1 + \xi)(m_t^2 + q^2\xi(1 + \xi)) \{M^2 + \xi(m_a^2 - q^2(1 + \xi))\}} \\
& \times \log \left(\frac{M^2}{m_a^2} \right) + \frac{2m_t^2 (m_a^4 - m_a^2 q^2(1 + \xi)^2 + 2q^4\xi(1 + \xi)^2) \log \left(\frac{M^2}{m_a^2} \right)}{q^2(q^2 - 4m_t^2)(1 + \xi) (m_t^2 + q^2\xi(1 + \xi)) (M^2 + \xi(m_a^2 - q^2(1 + \xi)))} \\
& + \frac{\xi (2m_a^4 - m_a^2 q^2(1 + \xi) + q^4(1 + \xi)^2(-1 + 2\xi))}{(q^2 - 4m_t^2)(m_t^2 + q^2\xi(1 + \xi))(M^2 + \xi(m_a^2 - q^2(1 + \xi)))} \log \left(\frac{M^2}{m_a^2} \right) \\
& + \frac{4m_a^2 (m_a^2 - q^2)}{q^2 (q^2 - 4m_t^2) (M^2 + \xi(m_a^2 - q^2(1 + \xi)))} \log \left(\frac{m_a^2}{m_a^2 - q^2} \right) \\
& - \frac{4q^2 (q^2 - 4m_t^2) \xi^2 \{M^4 + q^4\xi^3(1 + \xi) - M^2q^2\xi(1 + 2\xi)\}}{\{M^2 + \xi(m_a^2 - q^2(1 + \xi))\} \Lambda [m_t^2, q^2\xi^2, m_t^2 + q^2\xi(1 + \xi)]^2} \log \left(\frac{M^2}{M^2 - q^2\xi^2} \right) \\
& - \frac{2m_a^2 (m_a^2 - q^2)}{(4m_t^2 - q^2) \{M^2 + \xi(m_a^2 - q^2(1 + \xi))\}} f_2 [m_t^2, m_t^2, q^2, m_a, m_t, 0] \\
& + \frac{2q^4 (q^2 - 4m_t^2) \xi^3 (M^4 + q^4\xi^3(1 + \xi) - M^2q^2\xi(1 + 2\xi))}{\{M^2 + \xi(m_a^2 - q^2(1 + \xi))\} \Lambda [m_t^2, q^2\xi^2, m_t^2 + q^2\xi(1 + \xi)]^2} \\
& \times f_2 [m_t^2, q^2\xi^2, m_t^2 + q^2\xi(1 + \xi), m_t, 0, M] \\
& - \frac{2m_a^2 q^4 (q^2 - 4m_t^2) (1 + \xi)^4 \{M^2 - q^2(1 + \xi)^2 + m_a^2(1 + 2\xi)\}}{\{M^2 + \xi(m_a^2 - q^2(1 + \xi))\} \Lambda [m_t^2, q^2(1 + \xi)^2, m_t^2 + q^2\xi(1 + \xi)]^2}
\end{aligned}$$

$$\times f_2 \left[m_t^2, q^2(1+\xi)^2, m_t^2 + q^2\xi(1+\xi), m_t, m_a, M \right] \quad (\text{A.2})$$

$$\begin{aligned} \mathcal{F}_6(q^2) = & -\frac{2y_{att}^2 g_s^3 m_t}{(4\pi)^4} c_t \tilde{c}_t \int_0^1 dx \int_0^{1-x} dy \left[\frac{1}{y(y-1)} \right] \\ & \times \left[\frac{4m_t^2(1+\xi) f_1[m_t^2, m_t, m_a]}{\Lambda[m_t^2, q^2(1+\xi)^2, m_t^2 + q^2\xi(1+\xi)]} + \frac{2\{M^2 + \xi(m_a^2 - q^2(1+\xi))\}}{q^2(q^2 - 4m_t^2)\xi(1+\xi)} \log\left(\frac{m_t^2}{m_a^2}\right) \right. \\ & + \frac{2q^2(1+\xi)^2(-M^2 + q^2(1+\xi)^2 - m_a^2(1+2\xi)) f_1[q^2(1+\xi)^2, M, m_a]}{(M^2 + \xi(m_a^2 - q^2(1+\xi))) \Lambda[m_t^2, q^2(1+\xi)^2, m_t^2 + q^2\xi(1+\xi)]} \\ & + \frac{4q^2(q^2 - 4m_t^2)\xi(1+\xi)(m_t^2 + q^2\xi(1+\xi)) f_1[m_t^2 + q^2\xi(1+\xi), m_t, M]}{\Lambda[m_t^2, q^2\xi^2, m_t^2 + q^2\xi(1+\xi)] \Lambda[m_t^2, q^2(1+\xi)^2, m_t^2 + q^2\xi(1+\xi)]} \\ & - \frac{M^4(2+\xi) - 2M^2\xi(-m_a^2 + q^2(1+\xi)^2)}{q^2(q^2 - 4m_t^2)\xi(1+\xi)^2\{M^2 + \xi(m_a^2 - q^2(1+\xi))\}} \log\left(\frac{M^2}{m_a^2}\right) \\ & - \frac{\xi(-2m_a^2q^2(1+\xi)^2 + m_a^4(1+2\xi) + q^4(1+\xi)^2(1+\xi^2))}{q^2(q^2 - 4m_t^2)\xi(1+\xi)^2(M^2 + \xi(m_a^2 - q^2(1+\xi)))} \log\left(\frac{M^2}{m_a^2}\right) \\ & - \frac{2(m_a^2 - q^2)^2}{q^2(q^2 - 4m_t^2)(M^2 + \xi(m_a^2 - q^2(1+\xi)))} \log\left(\frac{m_a^2}{m_a^2 - q^2}\right) \\ & + \frac{2(M^2 - q^2\xi^2)^2}{\{M^2 + \xi(m_a^2 - q^2(1+\xi))\} \Lambda[m_t^2, q^2\xi^2, m_t^2 + q^2\xi(1+\xi)]} \log\left(\frac{M^2}{M^2 - q^2\xi^2}\right) \\ & - \frac{4m_t^2(m_a^2 - q^2)^2}{q^2(q^2 - 4m_t^2)(M^2 + \xi(m_a^2 - q^2(1+\xi)))} f_2[m_t^2, m_t^2, q^2, m_a, m_t, 0] \\ & - \frac{4m_t^2\xi(M^2 - q^2\xi^2)^2 f_2[m_t^2, q^2\xi^2, m_t^2 + q^2\xi(1+\xi), m_t, 0, M]}{\{M^2 + \xi(m_a^2 - q^2(1+\xi))\} \Lambda[m_t^2, q^2\xi^2, m_t^2 + q^2\xi(1+\xi)]} \\ & + \frac{4m_a^2q^2(1+\xi)^2 f_2[m_t^2, q^2(1+\xi)^2, m_t^2 + q^2\xi(1+\xi), m_t, m_a, M]}{\Lambda[m_t^2, q^2(1+\xi)^2, m_t^2 + q^2\xi(1+\xi)]} \\ & + \frac{4m_t^2(1+\xi)\{M^4 + (m_a^2 - q^2(1+\xi)^2)^2 - 2M^2(m_a^2 + q^2(1+\xi)^2)\}}{\{M^2 + \xi(m_a^2 - q^2(1+\xi))\} \Lambda[m_t^2, q^2(1+\xi)^2, m_t^2 + q^2\xi(1+\xi)]} \\ & \left. \times f_2[m_t^2, q^2(1+\xi)^2, m_t^2 + q^2\xi(1+\xi), m_t, m_a, M] \right] \quad (\text{A.3}) \end{aligned}$$

where we have used the following definitions:

$$\begin{aligned} \xi &= \frac{x}{y-1}, \quad M = \left[\frac{m_t^2}{y(1-y)} + \frac{q^2x(x+y-1)}{y(1-y)^2} \right]^{\frac{1}{2}}, \\ \Lambda[a, b, c] &= a^2 + b^2 + c^2 - 2ab - 2bc - 2ca. \end{aligned} \quad (\text{A.4})$$

The function $f_1[m_1, m_2, m_3]$ is given by

$$f_1[m_1, m_2, m_3] = \frac{\Lambda[m_1, m_2^2, m_3^2]}{m_1} \log\left(\frac{m_2^2 + m_3^2 - m_1 + \Lambda[m_1, m_2^2, m_3^2]}{2m_2m_3}\right). \quad (\text{A.5})$$

The function $f_2[s_1, s_2, s_3, m_1, m_2, m_3]$ is given by

$$\begin{aligned}
f_2[s_1, s_2, s_3, m_1, m_2, m_3] = & \frac{1}{\Lambda[s_1, s_2, s_3]} \\
& \left\{ -\text{Li}_2 \left[\frac{\Phi(s_1, s_2, s_3, m_1, m_2, m_3) - (m_1^2 - m_2^2 + s_1) \sqrt{\Lambda[s_1, s_2, s_3]}}{\Phi(s_1, s_2, s_3, m_1, m_2, m_3) - \sqrt{\Lambda[m_1^2, m_2^2, s_1] \Lambda[s_1, s_2, s_3]}} \right] \right. \\
& - i\epsilon s_1 \left(g_1(s_1, s_2, s_3) m_1^2 - g_2(s_1, s_2, s_3) m_2^2 + g_1(s_3, s_2, s_1) s_1 + 2m_3^2 s_1 \right) \\
& + \text{Li}_2 \left[\frac{\Phi(s_1, s_2, s_3, m_1, m_2, m_3) + (-m_1^2 + m_2^2 + s_1) \sqrt{\Lambda[s_1, s_2, s_3]}}{\Phi(s_1, s_2, s_3, m_1, m_2, m_3) - \sqrt{\Lambda[m_1^2, m_2^2, s_1] \Lambda[s_1, s_2, s_3]}} \right] \\
& - i\epsilon s_1 \left(g_1(s_1, s_2, s_3) m_1^2 - g_2(s_1, s_2, s_3) m_2^2 - g_2(s_2, s_1, s_3) s_1 + 2m_3^2 s_1 \right) \\
& - \text{Li}_2 \left[\frac{\Phi(s_1, s_2, s_3, m_1, m_2, m_3) - (m_1^2 - m_2^2 + s_1) \sqrt{\Lambda[s_1, s_2, s_3]}}{\Phi(s_1, s_2, s_3, m_1, m_2, m_3) + \sqrt{\Lambda[m_1^2, m_2^2, s_1] \Lambda[s_1, s_2, s_3]}} \right] \\
& + i\epsilon s_1 \left(g_1(s_1, s_2, s_3) m_1^2 - g_2(s_1, s_2, s_3) m_2^2 + g_1(s_3, s_2, s_1) s_1 + 2m_3^2 s_1 \right) \\
& + \text{Li}_2 \left[\frac{\Phi(s_1, s_2, s_3, m_1, m_2, m_3) + (-m_1^2 + m_2^2 + s_1) \sqrt{\Lambda[s_1, s_2, s_3]}}{\Phi(s_1, s_2, s_3, m_1, m_2, m_3) + \sqrt{\Lambda[m_1^2, m_2^2, s_1] \Lambda[s_1, s_2, s_3]}} \right] \\
& + i\epsilon s_1 \left(g_1(s_1, s_2, s_3) m_1^2 - g_2(s_1, s_2, s_3) m_2^2 - g_2(s_2, s_1, s_3) s_1 + 2m_3^2 s_1 \right) \\
& - \text{Li}_2 \left[\frac{\Phi(s_3, s_2, s_1, m_1, m_3, m_2) + (m_1^2 - m_3^2 - s_3) \sqrt{\Lambda[s_1, s_2, s_3]}}{\Phi(s_3, s_2, s_1, m_1, m_3, m_2) + \sqrt{\Lambda[m_1^2, m_3^2, s_3] \Lambda[s_1, s_2, s_3]}} \right] \\
& + i\epsilon s_3 \left(-g_2(s_2, s_1, s_3) m_1^2 - g_2(s_1, s_2, s_3) m_3^2 + g_1(s_1, s_2, s_3) s_3 + 2m_2^2 s_3 \right) \\
& + \text{Li}_2 \left[\frac{\Phi(s_3, s_2, s_1, m_1, m_3, m_2) + (m_1^2 - m_3^2 + s_3) \sqrt{\Lambda[s_1, s_2, s_3]}}{\Phi(s_3, s_2, s_1, m_1, m_3, m_2) + \sqrt{\Lambda[m_1^2, m_3^2, s_3] \Lambda[s_1, s_2, s_3]}} \right] \\
& + i\epsilon s_3 \left(-g_2(s_2, s_1, s_3) m_1^2 - g_2(s_1, s_2, s_3) m_3^2 - g_2(s_1, s_3, s_2) s_3 + 2m_2^2 s_3 \right) \\
& + \text{Li}_2 \left[\frac{-\Phi(s_3, s_2, s_1, m_1, m_3, m_2) - (m_1^2 - m_3^2 + s_3) \sqrt{\Lambda[s_1, s_2, s_3]}}{-\Phi(s_3, s_2, s_1, m_1, m_3, m_2) + \sqrt{\Lambda[m_1^2, m_3^2, s_3] \Lambda[s_1, s_2, s_3]}} \right] \\
& - i\epsilon s_3 \left(-g_2(s_2, s_1, s_3) m_1^2 - g_2(s_1, s_2, s_3) m_3^2 - g_2(s_1, s_3, s_2) s_3 + 2m_2^2 s_3 \right) \\
& - \text{Li}_2 \left[\frac{-\Phi(s_3, s_2, s_1, m_1, m_3, m_2) + (-m_1^2 + m_3^2 + s_3) \sqrt{\Lambda[s_1, s_2, s_3]}}{-\Phi(s_3, s_2, s_1, m_1, m_3, m_2) + \sqrt{\Lambda[m_1^2, m_3^2, s_3] \Lambda[s_1, s_2, s_3]}} \right]
\end{aligned}$$

$$\begin{aligned}
& - i\epsilon s_3 \left(-g_2(s_2, s_1, s_3)m_1^2 - g_2(s_1, s_2, s_3)m_3^2 + g_1(s_1, s_2, s_3)s_3 + 2m_2^2 s_3 \right) \Big] \\
& - \text{Li}_2 \left[\frac{\Phi(s_2, s_1, s_3, m_3, m_2, m_1) - (m_2^2 - m_3^2 + s_2) \sqrt{\Lambda[s_1, s_2, s_3]}}{\Phi(s_2, s_1, s_3, m_3, m_2, m_1) + \sqrt{\Lambda[m_2^2, m_3^2, s_2]\Lambda[s_1, s_2, s_3]}} \right] \\
& + i\epsilon s_2 \left(g_1(s_3, s_2, s_1)m_2^2 - g_2(s_1, s_2, s_3)m_3^2 - g_2(s_1, s_2, s_3)s_2 + 2m_1^2 s_2 \right) \Big] \\
& + \text{Li}_2 \left[\frac{\Phi(s_2, s_1, s_3, m_3, m_2, m_1) + (-m_2^2 + m_3^2 + s_2) \sqrt{\Lambda[s_1, s_2, s_3]}}{\Phi(s_2, s_1, s_3, m_3, m_2, m_1) + \sqrt{\Lambda[m_2^2, m_3^2, s_2]\Lambda[s_1, s_2, s_3]}} \right] \\
& + i\epsilon s_2 \left(g_1(s_3, s_2, s_1)m_2^2 - g_2(s_1, s_2, s_3)m_3^2 - g_2(s_1, s_2, s_3)s_2 + 2m_1^2 s_2 \right) \Big] \\
& + \text{Li}_2 \left[\frac{-\Phi(s_2, s_3, s_1, m_2, m_3, m_1) + (m_2^2 - m_3^2 - s_2) \sqrt{\Lambda[s_1, s_2, s_3]}}{-\Phi(s_2, s_3, s_1, m_2, m_3, m_1) + \sqrt{\Lambda[m_2^2, m_3^2, s_2]\Lambda[s_1, s_2, s_3]}} \right] \\
& - i\epsilon s_2 \left(g_1(s_3, s_2, s_1)m_2^2 - g_2(s_1, s_2, s_3)m_3^2 - g_2(s_1, s_2, s_3)s_2 + 2m_1^2 s_2 \right) \Big] \\
& - \text{Li}_2 \left[\frac{-\Phi(s_2, s_3, s_1, m_2, m_3, m_1) + (m_2^2 - m_3^2 + s_2) \sqrt{\Lambda[s_1, s_2, s_3]}}{-\Phi(s_2, s_3, s_1, m_2, m_3, m_1) + \sqrt{\Lambda[m_2^2, m_3^2, s_2]\Lambda[s_1, s_2, s_3]}} \right] \\
& - i\epsilon s_2 \left(g_1(s_3, s_2, s_1)m_2^2 - g_2(s_1, s_2, s_3)m_3^2 - g_2(s_1, s_2, s_3)s_2 + 2m_1^2 s_2 \right) \Big] \Big\} , \quad (\text{A.6})
\end{aligned}$$

where $\Phi(s_1, s_2, s_3, m_1, m_2, m_3) = m_1^2(s_1 + s_2 - s_3) + m_2^2(s_1 - s_2 + s_3) + s_1(-2m_3^2 - s_1 + s_2 + s_3)$, $g_1(s_1, s_2, s_3) = -s_1 - s_2 + s_3 + \sqrt{\Lambda[s_1, s_2, s_3]}$, and $g_2(s_1, s_2, s_3) = s_1 - s_2 + s_3 + \sqrt{\Lambda[s_1, s_2, s_3]}$. The dilogarithm is defined as follows:

$$\text{Li}_2(z) = - \int_0^z \frac{\log(1-t)}{t} dt \quad \text{for } z \in \mathbb{C} . \quad (\text{A.7})$$

References

- [1] R. D. Peccei and H. R. Quinn, *CP Conservation in the Presence of Instantons*, *Phys. Rev. Lett.* **38** (1977) 1440.
- [2] R. D. Peccei and H. R. Quinn, *Constraints Imposed by CP Conservation in the Presence of Instantons*, *Phys. Rev. D* **16** (1977) 1791.
- [3] S. Weinberg, *A New Light Boson?*, *Phys. Rev. Lett.* **40** (1978) 223.
- [4] F. Wilczek, *Problem of Strong P and T Invariance in the Presence of Instantons*, *Phys. Rev. Lett.* **40** (1978) 279.
- [5] J. Preskill, M. B. Wise and F. Wilczek, *Cosmology of the Invisible Axion*, *Phys. Lett. B* **120** (1983) 127.
- [6] L. F. Abbott and P. Sikivie, *A Cosmological Bound on the Invisible Axion*, *Phys. Lett. B* **120** (1983) 133.

- [7] M. Dine and W. Fischler, *The Not So Harmless Axion*, *Phys. Lett. B* **120** (1983) 137.
- [8] R. L. Davis, *Cosmic Axions from Cosmic Strings*, *Phys. Lett. B* **180** (1986) 225.
- [9] A. Davidson and K. C. Wali, *MINIMAL FLAVOR UNIFICATION VIA MULTIGENERATIONAL PECCEI-QUINN SYMMETRY*, *Phys. Rev. Lett.* **48** (1982) 11.
- [10] F. Wilczek, *Axions and Family Symmetry Breaking*, *Phys. Rev. Lett.* **49** (1982) 1549.
- [11] Y. Ema, K. Hamaguchi, T. Moroi and K. Nakayama, *Flaxion: a minimal extension to solve puzzles in the standard model*, *JHEP* **01** (2017) 096 [[1612.05492](#)].
- [12] L. Calibbi, F. Goertz, D. Redigolo, R. Ziegler and J. Zupan, *Minimal axion model from flavor*, *Phys. Rev. D* **95** (2017) 095009 [[1612.08040](#)].
- [13] P. W. Graham, D. E. Kaplan and S. Rajendran, *Cosmological Relaxation of the Electroweak Scale*, *Phys. Rev. Lett.* **115** (2015) 221801 [[1504.07551](#)].
- [14] J. Jaeckel and A. Ringwald, *The Low-Energy Frontier of Particle Physics*, *Ann. Rev. Nucl. Part. Sci.* **60** (2010) 405 [[1002.0329](#)].
- [15] D. J. E. Marsh, *Axion Cosmology*, *Phys. Rept.* **643** (2016) 1 [[1510.07633](#)].
- [16] I. G. Irastorza and J. Redondo, *New experimental approaches in the search for axion-like particles*, *Prog. Part. Nucl. Phys.* **102** (2018) 89 [[1801.08127](#)].
- [17] L. Di Luzio, M. Giannotti, E. Nardi and L. Visinelli, *The landscape of QCD axion models*, *Phys. Rept.* **870** (2020) 1 [[2003.01100](#)].
- [18] B. Döbrich, J. Jaeckel and T. Spadaro, *Light in the beam dump - ALP production from decay photons in proton beam-dumps*, *JHEP* **05** (2019) 213 [[1904.02091](#)].
- [19] J. Jaeckel and M. Spannowsky, *Probing MeV to 90 GeV axion-like particles with LEP and LHC*, *Phys. Lett. B* **753** (2016) 482 [[1509.00476](#)].
- [20] S. Knapen, T. Lin, H. K. Lou and T. Melia, *Searching for Axionlike Particles with Ultraperipheral Heavy-Ion Collisions*, *Phys. Rev. Lett.* **118** (2017) 171801 [[1607.06083](#)].
- [21] I. Brivio, M. B. Gavela, L. Merlo, K. Mimasu, J. M. No, R. del Rey et al., *ALPs Effective Field Theory and Collider Signatures*, *Eur. Phys. J. C* **77** (2017) 572 [[1701.05379](#)].
- [22] A. Mariotti, D. Redigolo, F. Sala and K. Tobioka, *New LHC bound on low-mass diphoton resonances*, *Phys. Lett. B* **783** (2018) 13 [[1710.01743](#)].
- [23] X. Cid Vidal, A. Mariotti, D. Redigolo, F. Sala and K. Tobioka, *New Axion Searches at Flavor Factories*, *JHEP* **01** (2019) 113 [[1810.09452](#)].
- [24] D. Aloni, Y. Soreq and M. Williams, *Coupling QCD-Scale Axionlike Particles to Gluons*, *Phys. Rev. Lett.* **123** (2019) 031803 [[1811.03474](#)].
- [25] D. Aloni, C. Fanelli, Y. Soreq and M. Williams, *Photoproduction of Axionlike Particles*, *Phys. Rev. Lett.* **123** (2019) 071801 [[1903.03586](#)].
- [26] M. Bauer, M. Neubert and A. Thamm, *Collider Probes of Axion-Like Particles*, *JHEP* **12** (2017) 044 [[1708.00443](#)].
- [27] M. Bauer, M. Neubert and A. Thamm, *LHC as an Axion Factory: Probing an Axion Explanation for $(g-2)_\mu$ with Exotic Higgs Decays*, *Phys. Rev. Lett.* **119** (2017) 031802 [[1704.08207](#)].

- [28] W. J. Marciano, A. Masiero, P. Paradisi and M. Passera, *Contributions of axionlike particles to lepton dipole moments*, *Phys. Rev. D* **94** (2016) 115033 [[1607.01022](#)].
- [29] J. E. Moody and F. Wilczek, *NEW MACROSCOPIC FORCES?*, *Phys. Rev. D* **30** (1984) 130.
- [30] M. Pospelov, *CP odd interaction of axion with matter*, *Phys. Rev. D* **58** (1998) 097703 [[hep-ph/9707431](#)].
- [31] G. Raffelt, *Limits on a CP-violating scalar axion-nucleon interaction*, *Phys. Rev. D* **86** (2012) 015001 [[1205.1776](#)].
- [32] S. Bertolini, L. Di Luzio and F. Nesti, *Axion-mediated forces, CP violation and left-right interactions*, *Phys. Rev. Lett.* **126** (2021) 081801 [[2006.12508](#)].
- [33] C. A. J. O'Hare and E. Vitagliano, *Cornering the axion with CP-violating interactions*, *Phys. Rev. D* **102** (2020) 115026 [[2010.03889](#)].
- [34] Y. V. Stadnik, V. A. Dzuba and V. V. Flambaum, *Improved Limits on Axionlike-Particle-Mediated P, T -Violating Interactions between Electrons and Nucleons from Electric Dipole Moments of Atoms and Molecules*, *Phys. Rev. Lett.* **120** (2018) 013202 [[1708.00486](#)].
- [35] V. A. Dzuba, V. V. Flambaum, I. B. Samsonov and Y. V. Stadnik, *New constraints on axion-mediated P,T-violating interaction from electric dipole moments of diamagnetic atoms*, *Phys. Rev. D* **98** (2018) 035048 [[1805.01234](#)].
- [36] L. Di Luzio, R. Gröber and P. Paradisi, *Hunting for CP-violating axionlike particle interactions*, *Phys. Rev. D* **104** (2021) 095027 [[2010.13760](#)].
- [37] LHC HIGGS CROSS SECTION WORKING GROUP collaboration, J. R. Andersen et al., *Handbook of LHC Higgs Cross Sections: 3. Higgs Properties*, [1307.1347](#).
- [38] C.-S. Huang and T.-J. Li, *Electric dipole moment and chromoelectric electric dipole moment of the top quark in $SU(3)(C) \times SU(3)(L) \times U(1)(X)$ model*, *Z. Phys. C* **68** (1995) 319.
- [39] T. Ibrahim and P. Nath, *The Chromoelectric Dipole Moment of the Top Quark in Models with Vector Like Multiplets*, *Phys. Rev. D* **84** (2011) 015003 [[1104.3851](#)].
- [40] A. Aboubrahim, T. Ibrahim, P. Nath and A. Zorik, *Chromoelectric Dipole Moments of Quarks in MSSM Extensions*, *Phys. Rev. D* **92** (2015) 035013 [[1507.02668](#)].
- [41] M. Gorbahn and U. Haisch, *Searching for $t \rightarrow c(u)h$ with dipole moments*, *JHEP* **06** (2014) 033 [[1404.4873](#)].
- [42] A. I. Hernández-Juárez, A. Moyotl and G. Tavares-Velasco, *Chromomagnetic and chromoelectric dipole moments of the top quark in the fourth-generation THDM*, *Phys. Rev. D* **98** (2018) 035040 [[1805.00615](#)].
- [43] A. I. Hernández-Juárez, G. Tavares-Velasco and A. Moyotl, *Chromomagnetic and chromoelectric dipole moments of quarks in the reduced 331 model*, *Chin. Phys. C* **45** (2021) 113101 [[2012.09883](#)].
- [44] H. Gisbert, V. Miralles and J. Ruiz-Vidal, *Electric dipole moments from colour-octet scalars*, *JHEP* **04** (2022) 077 [[2111.09397](#)].
- [45] M. Aiko, M. Endo, S. Kanemura and Y. Mura, *Electroweak baryogenesis in 2HDM without EDM cancellation*, [2504.07705](#).

- [46] T. Abe, J. Hisano, T. Kitahara and K. Tobioka, *Gauge invariant Barr-Zee type contributions to fermionic EDMs in the two-Higgs doublet models*, *JHEP* **01** (2014) 106 [[1311.4704](#)].
- [47] Y. T. Chien, V. Cirigliano, W. Dekens, J. de Vries and E. Mereghetti, *Direct and indirect constraints on CP-violating Higgs-quark and Higgs-gluon interactions*, *JHEP* **02** (2016) 011 [[1510.00725](#)].
- [48] Y. Nakai and M. Reece, *Electric Dipole Moments in Natural Supersymmetry*, *JHEP* **08** (2017) 031 [[1612.08090](#)].
- [49] CMS collaboration, A. M. Sirunyan et al., *Measurement of the top quark forward-backward production asymmetry and the anomalous chromoelectric and chromomagnetic moments in pp collisions at $\sqrt{s} = 13$ TeV*, *JHEP* **06** (2020) 146 [[1912.09540](#)].
- [50] J. Hisano, K. Tsumura and M. J. S. Yang, *QCD Corrections to Neutron Electric Dipole Moment from Dimension-six Four-Quark Operators*, *Phys. Lett. B* **713** (2012) 473 [[1205.2212](#)].
- [51] F. Maltoni, D. Pagani and S. Tentori, *Top-quark pair production as a probe of light top-philic scalars and anomalous Higgs interactions*, *JHEP* **09** (2024) 098 [[2406.06694](#)].
- [52] L. Di Luzio, H. Gisbert, G. Levati, P. Paradisi and P. Sørensen, *CP-Violating Axions: A Theory Review*, [2312.17310](#).
- [53] L. Di Luzio, G. Levati and P. Paradisi, *The chiral Lagrangian of CP-violating axion-like particles*, *JHEP* **02** (2024) 020 [[2311.12158](#)].
- [54] Q.-H. Cao, J.-N. Fu, Y. Liu, X.-H. Wang and R. Zhang, *Probing top-philic new physics via four-top-quark production*, *Chin. Phys. C* **45** (2021) 093107 [[2105.03372](#)].
- [55] S. Blasi, F. Maltoni, A. Mariotti, K. Mimasu, D. Pagani and S. Tentori, *Top-philic ALP phenomenology at the LHC: the elusive mass-window*, *JHEP* **06** (2024) 077 [[2311.16048](#)].
- [56] S. Tentori, *Top-philic ALP phenomenology at the LHC*, in *16th International Workshop on Top Quark Physics*, 1, 2024, [2401.05068](#).
- [57] S. Weinberg, *Larger Higgs Exchange Terms in the Neutron Electric Dipole Moment*, *Phys. Rev. Lett.* **63** (1989) 2333.
- [58] J. F. Gunion and D. Wyler, *Inducing a large neutron electric dipole moment via a quark chromoelectric dipole moment*, *Phys. Lett. B* **248** (1990) 170.
- [59] P. Haberl, O. Nachtmann and A. Wilch, *Top production in hadron hadron collisions and anomalous top - gluon couplings*, *Phys. Rev. D* **53** (1996) 4875 [[hep-ph/9505409](#)].
- [60] J. F. Kamenik, M. Papucci and A. Weiler, *Constraining the dipole moments of the top quark*, *Phys. Rev. D* **85** (2012) 071501 [[1107.3143](#)].
- [61] W. Bernreuther and Z.-G. Si, *Top quark spin correlations and polarization at the LHC: standard model predictions and effects of anomalous top chromo moments*, *Phys. Lett. B* **725** (2013) 115 [[1305.2066](#)].
- [62] CMS collaboration, V. Khachatryan et al., *Measurements of $t\bar{t}$ spin correlations and top quark polarization using dilepton final states in pp collisions at $\sqrt{s} = 8$ TeV*, *Phys. Rev. D* **93** (2016) 052007 [[1601.01107](#)].
- [63] I. D. Choudhury and A. Lahiri, *Anomalous chromomagnetic moment of quarks*, *Mod. Phys. Lett. A* **30** (2015) 1550113 [[1409.0073](#)].

- [64] R. Bermudez, L. Albino, L. X. Gutiérrez-Guerrero, M. E. Tejeda-Yeomans and A. Bashir, *Quark-gluon Vertex: A Perturbation Theory Primer and Beyond*, *Phys. Rev. D* **95** (2017) 034041 [[1702.04437](#)].
- [65] R. Martinez, M. A. Perez and N. Poveda, *Chromomagnetic Dipole Moment of the Top Quark Revisited*, *Eur. Phys. J. C* **53** (2008) 221 [[hep-ph/0701098](#)].
- [66] A. Czarnecki and B. Krause, *Neutron electric dipole moment in the standard model: Valence quark contributions*, *Phys. Rev. Lett.* **78** (1997) 4339 [[hep-ph/9704355](#)].
- [67] PARTICLE DATA GROUP collaboration, P. A. Zyla et al., *Review of Particle Physics*, *PTEP* **2020** (2020) 083C01.
- [68] S. M. Barr and A. Zee, *Electric Dipole Moment of the Electron and of the Neutron*, *Phys. Rev. Lett.* **65** (1990) 21.
- [69] S. Bisal, *Two-loop contributions to the anomalous chromomagnetic dipole moment of the top quark in two-Higgs-doublet models*, *Phys. Lett. B* **855** (2024) 138848 [[2404.14065](#)].
- [70] S. Bisal, D. Das, S. Majhi and S. Mitra, *Production of singlet dominated scalar(s) at the LHC*, *Phys. Lett. B* **839** (2023) 137806 [[2207.01358](#)].
- [71] G. Degrandi, E. Franco, S. Marchetti and L. Silvestrini, *QCD corrections to the electric dipole moment of the neutron in the MSSM*, *JHEP* **11** (2005) 044 [[hep-ph/0510137](#)].
- [72] E. Braaten, C.-S. Li and T.-C. Yuan, *The Evolution of Weinberg’s Gluonic CP Violation Operator*, *Phys. Rev. Lett.* **64** (1990) 1709.
- [73] D. Chang, T. W. Kephart, W.-Y. Keung and T. C. Yuan, *The Chromoelectric dipole moment of the heavy quark and purely gluonic CP violating operators*, *Phys. Rev. Lett.* **68** (1992) 439.
- [74] C. Abel et al., *Measurement of the Permanent Electric Dipole Moment of the Neutron*, *Phys. Rev. Lett.* **124** (2020) 081803 [[2001.11966](#)].
- [75] B. Graner, Y. Chen, E. G. Lindahl and B. R. Heckel, *Reduced Limit on the Permanent Electric Dipole Moment of Hg199*, *Phys. Rev. Lett.* **116** (2016) 161601 [[1601.04339](#)].
- [76] M. Pospelov and A. Ritz, *Electric dipole moments as probes of new physics*, *Annals Phys.* **318** (2005) 119 [[hep-ph/0504231](#)].
- [77] V. Cirigliano, A. Crivellin, W. Dekens, J. de Vries, M. Hoferichter and E. Mereghetti, *CP Violation in Higgs-Gauge Interactions: From Tabletop Experiments to the LHC*, *Phys. Rev. Lett.* **123** (2019) 051801 [[1903.03625](#)].
- [78] D. A. Demir, M. Pospelov and A. Ritz, *Hadronic EDMs, the Weinberg operator, and light gluinos*, *Phys. Rev. D* **67** (2003) 015007 [[hep-ph/0208257](#)].
- [79] F. Esser, M. Madigan, V. Sanz and M. Ubiali, *On the coupling of axion-like particles to the top quark*, *JHEP* **09** (2023) 063 [[2303.17634](#)].
- [80] S. Carra, V. Goumarre, R. Gupta, S. Heim, B. Heinemann, J. Kuechler et al., *Constraining off-shell production of axionlike particles with $Z\gamma$ and WW differential cross-section measurements*, *Phys. Rev. D* **104** (2021) 092005 [[2106.10085](#)].
- [81] M. B. Gavela, J. M. No, V. Sanz and J. F. de Trocóniz, *Nonresonant Searches for Axionlike Particles at the LHC*, *Phys. Rev. Lett.* **124** (2020) 051802 [[1905.12953](#)].
- [82] CMS collaboration, A. Tumasyan et al., *Search for heavy resonances decaying to ZZ or ZW and axion-like particles mediating nonresonant ZZ or ZH production at $\sqrt{s} = 13$ TeV*, *JHEP* **04** (2022) 087 [[2111.13669](#)].

- [83] NA62 collaboration, E. Cortina Gil et al., *Measurement of the very rare $K^+ \rightarrow \pi^+ \nu \bar{\nu}$ decay*, *JHEP* **06** (2021) 093 [[2103.15389](#)].
- [84] BABAR collaboration, J. P. Lees et al., *Search for $B \rightarrow K^{(*)} \nu \bar{\nu}$ and invisible quarkonium decays*, *Phys. Rev. D* **87** (2013) 112005 [[1303.7465](#)].
- [85] A. V. Phan and S. Westhoff, *Precise tests of the axion coupling to tops*, *JHEP* **05** (2024) 075 [[2312.00872](#)].
- [86] ATLAS collaboration, G. Aad et al., *Search for a new pseudoscalar decaying into a pair of muons in events with a top-quark pair at $\sqrt{s}=13$ TeV with the ATLAS detector*, *Phys. Rev. D* **108** (2023) 092007 [[2304.14247](#)].
- [87] CMS collaboration, A. M. Sirunyan et al., *Search for physics beyond the standard model in multilepton final states in proton-proton collisions at $\sqrt{s} = 13$ TeV*, *JHEP* **03** (2020) 051 [[1911.04968](#)].
- [88] S. Bruggisser, L. Grabitz and S. Westhoff, *Global analysis of the ALP effective theory*, *JHEP* **01** (2024) 092 [[2308.11703](#)].